Chinese Herbal Medicines 17 (2025) 392–403

Contents lists available at ScienceDirect

Chinese Herbal Medicines

journal homepage: www.elsevier.com/locate/chmed

Original Article

Overexpression of SULT1E1 alleviates salt-processed *Psoraleae Fructus*-induced cholestatic liver damage

Yu Wu [a,b,1], Yan Xu [b,1], Hao Cai [b], Zhengying Hua [b], Meimei Luo [b], Letao Hu [b], Nong Zhou [b,c], Xinghong Wang [a,*], Weidong Li [b,*]

[a] *Nantong Hospital of Traditional Chinese Medicine, Affiliated Traditional Chinese Medicine Hospital of Nantong University, Nantong 226000, China*
[b] *Jiangsu Key Laboratory of Chinese Medicine Processing, Engineering Center of State Ministry of Education for Standardization of Chinese Medicine Processing, Nanjing University of Chinese Medicine, Nanjing 210023, China*
[c] *Chongqing Engineering Laboratory of Green Planting and Deep Processing of Famous-region Drug in the Three Gorges Reservoir Region, College of Biology and Food Engineering, Chongqing Three Gorges University, Chongqing 404120, China*

ARTICLE INFO

Article history:
Received 30 January 2024
Revised 19 July 2024
Accepted 7 November 2024
Available online 12 November 2024

Keywords:
cholestatic liver damage
FXR-SULT1E1 signaling
isopsoralen
psoralen
rAAV8-SULT1E1
salt-processed *Psoraleae Fructus*

ABSTRACT

Objective: Salt-processed *Psoraleae Fructus* (SPF) is widely used as a phytoestrogen-like agent in the treatment of osteoporosis. However, due to improper clinical use or misuse, resulting in liver damage. In this study, network pharmacology was employed to analyze the mechanism of cholestatic liver damage. An adeno-associated virus overexpressing SULT1E1 (rAAV8-SULT1E1) was constructed and the hepatotoxicity of SPF, psoralen, and isopsoralen was determined.

Methods: By utilizing three databases inclding TCMSP, TCMID, and BATMAN- TCM, the targets of the three databases were summarized, and a total of 45 psoralen compounds were included. Network pharmacology analysis was then performed. The adenoviral vectors were injected into the tail vein of C57BL6 mice to elucidate the role of SULT1E1 in SPF-induced cholestasis-mediated hepatotoxicity *in vivo*. SPF (10 g/kg), psoralen, and isopsoralen (50 mg/kg each) were intragastrically administered to mice for 30 d. B-ultrasound and samples were collected and examined for follow-up experiments.

Results: A total of 854 targets were predicted for 45 active components, with 151 cholestasis-mediated hepatotoxicity-related disease targets obtained for SPF. A total of 126 pathways were enriched based on KEGG pathway analysis, with the "estrogen signaling pathway" identified as one of the top 20 pathways. In terms of pathological hepatic changes, treated mice had visually swollen hepatocytes, dilated bile ducts, and elevated serum biochemical markers, which were more prominent in mice treated with isopsoralen than in those treated with other compounds. Notably, the overexpression of SULT1E1 could reverse liver damage in each treatment group. B-ultrasound was used to observe the size of the gallbladder *in vivo*. The size of the gallbladder was found to significantly increase on day 30 after treatment in the SPF-, psoralen-, and isopsoralen-treated groups, especially the SPF group. Compared with the expression levels in the negative control group (rAAV8-empty + con), the expression levels of FXR, Mrp2, Bsep, SULT1E1, SULT2A1, Ntcp, and Nrf2 decreased, whereas those of CYP7a1 and IL-6 increased in the SPF-, psoralen-, and isopsoralen-treated groups.

Conclusion: The overexpression of SULT1E1 could alleviate the decreased or increased expression of indicators, indicating that SULT1E1 is an important target gene for SPF-induced liver damage. The severity of liver damage was significantly lower in the rAAV8-SULT1E1 groups than in the rAAV8-empty groups.

1. Introduction

Psoraleae Fructus (Buguzhi in Chinese) has been commonly used as a tonic in China for centuries, serving as a dietary upplement to treat skin diseases, such as vitiligo and psoriasis (Chinese Pharmacopeia Commission, 2025). Salt-processed *Psoraleae Fructus* (SPF) is widely distributed and used as an alternative natural remedy due to its varying bioactivities. SPF acts as an estrogen upplement and an antimicrobial, antioxidant, and antitumor compound that ameliorates the symptoms of diarrhea, osteoporosis, and depression (Chopra, Dhingra, & Dhar, 2013). In recent years, numerous studies have reported adverse reactions to SPF, especially liver damage. Some efforts have been dedicated to elucidating the

* Corresponding authors.
E-mail addresses: 180661484@qq.com (X. Wang), liweidong0801@163.com (W. Li).
[1] These authors contributed equally to this study.

https://doi.org/10.1016/j.chmed.2024.11.002
1674-6384/

hepatotoxicity mechanism of PF, which involves bile acid (BA) metabolism, transport disorders, oxidative stress, mitochondrial damage, the inhibition of liver cell regeneration and repair, and inflammatory reaction (Shi et al., 2022). Psoralen and isopsoralen induce liver toxicity by inhibiting BA excretion, which induces the accumulation of toxins in the hepatocytes (Wang et al., 2019). Bakuchiol, psoralen, and isopsoralen exert substantial plant estrogenic activities (Xin et al., 2010; Lim, Ha, Ahn, & Kim, 2011; Xu et al., 2019). Excessive levels of estrogen-like phytochemicals can cause liver damage (Choi & Song, 2009). The acute oral toxicity test of an ethanol extract of SPF revealed that 107 compounds, including psoralen and isopsoralen, were toxic ingredients, with the liver and kidney as its main target organs (Gao et al., 2023).

Farnesoid X receptor (FXR) is involved in the primary regulatory mechanism associated with promoting BA homeostasis and the pathogenesis of cholestasis. FXR regulates the hepatobiliary transport of BAs and can induce the expression of efflux transporters located at the canalicular membrane of hepatocytes (Kleven, Gomes, Wortham, Enns, & Kahl, 2018). The liver is a major metabolic organ. Therefore, the expression of genes in the liver is an invaluable tool for metabolic studies and gene therapy. By employing quantitative proteomics and metabolomics analysis, Duan et al. (2020) found that the alteration of BA metabolism was markedly associated with liver damage induced by PF. Coumarins in PF are involved in multiple pathways, and monoterpene phenols play a role in BA transporters. The upstream molecules induced by coumarins include the recombinant FXR and protein kinase RNA-like ER kinase (PERK) (Shi et al., 2022). However, the factors that trigger SPF-induced liver damage remain unclear.

Recombinant adeno-associated virus (rAAV) vectors of serotype 8 (AAV8) efficiently transduce muscle, liver, and brain tissues (Zincarelli, Soltys, Rengo, & Rabinowitz, 2008; Wang et al., 2015). Therefore, the effect of tail vein injection of adeno-associated virus overexpressing sulfotransferase family 1E member 1 (SULT1E1) on SPF-induced cholestatic liver damage in mice was the objective of this study.

2. Materials and methods

2.1. Materials and reagents

SPF was purchased from the Bozhou traditional Chinese medicine market (Anhui, China). The specimens were validated by Professor Jianwei Chen (Nanjing University of Chinese Medicine). Voucher specimens (No. 1804058) were deposited in the herbarium at the Nanjing University of Chinese Medicine (Nanjing, China). Alanine transaminase (ALT; C009-1), aspartate aminotransferase (AST; C010-1), alkaline phosphatase (ALP; C059-1), and total bilirubin determination kits (C019-1) were obtained from Nanjing Jiancheng Institute of Biotechnology (Nanjing, China).

2.2. Prediction of active component targets and screening of disease targets

The TCMSP web tool was used to predict the potential targets related to the main active ingredients, with oral bioavailability (OB) $\geq$ 20% and drug-like (DL) $\geq$ 0.1 as the criteria (Liao, Zhao, & Guo, 2024). Components not found in the TCMSP database were screened using the TCMID and Batman-TCM databases, with a score $\geq$ 15 as the standard. Thereafter, the active components were obtained. Species were qualified as human species using Uniprot database. Drug-induced cholestasis was searched in the GeneCards and OMIM databases to obtain the target genes related to drug-induced cholestasis.

2.3. Protein–protein interactions and compound target network construction

The targets of SPF were intersected with the targets of drug-induced cholestasis, and the cross targets were considered as putative targets of SPF in cholestatic liver damage. A Venn diagram was then generated using the "Venn Diagram" Package, and the intersection targets were imported into the Cytoscape database to obtain the interaction relationship between the targets. A "drug-component-disease-target" network was also constructed, and the intersection targets were imported into the Cytoscape database to obtain the interaction relationship between the targets and establish a PPI network.

2.4. Gene ontology and Kyoto Encyclopedia of Genes and Genomes pathway enrichment analyses

Gene ontology (GO) and Kyoto Encyclopedia of Genes and Genomes (KEGG) pathway enrichment analyses were performed using the OmicShare tools (www.omicshare.com/tools). An adjusted P value <0.05 indicated statistical significance. The top 20 enriched pathways are displayed using a bubble map.

2.5. HPLC fingerprint

The SPF decoction was directly determined using the following conditions: column, Kromasil 100–5-C_{18} chromatographic column (4.6 mm $\times$ 250 mm, 5 μm); column temperature, 30 °C; flow rate, 1.0 mL/min; sample volume, 10 μL; and detection wavelength, 246 nm. The mobile phase consisted of acetonitrile (A) and 0.1% formic acid aqueous solution (B), and the following gradient elution was employed: 0–5.0 min (10–20% A), 5.0–20.0 min (20–40% A), 20.0–30.0 min (40–45% A), 30.0–40.0 min (45–60% A), 40.0–50.0 min (60–95% A), 50.0–55.0 min (95% A), and 55.0–70.0 min (95–10% A).

2.6. Animals

C57BL6 mice (12 weeks; weight 18–22 g; n = 54) were acquired from Shanghai Slack Laboratory Animal Co., Ltd. (Qualified number: 20170005051699). All animals received humane care and were housed in animal laboratory facilities under adequate temperature and humidity and sufficient light. All treatment protocols were performed in accordance with the provision and general recommendations of the Chinese legislation regarding experimental animals. The experiment was approved by the Animal Care and Ethics Committee of Nanjing University of Chinese medicine (202004A057).

2.7. Production of adeno-associated viral vector

Vectors were prepared using a two-plasmid co-transfection method. The vectors were eluted from the column using 215 mmol/L NaCl (pH 8.0), and the vector-containing fractions were collected, pooled, and concentrated. A Biomax 100 K concentrator (Millipore) was used to buffer exchange the solution into Alcon BSS PLUS irrigating solution with 0.014 % Tween 20. The titer of the DNase-resistant vector genomes was measured using real-time PCR relative to a standard. The viral titers were determined via quantitative PCR using SULT1E1 primers(forward:5′-TGCTTTC TGAGAGAGGATCCCGCCACCATGGAGACTTCTATGCCTGAG-3′;reverse: 5′-CTCACATGGTGGCGGGATCCTCGAGCTCCATTCTAAACTTCACAGTG-3′). Finally, the purity of the vector was validated using silver-stained SDS-PAGE, assayed for sterility and lack of endotoxin, and then aliquoted and stored at −80 °C.

2.8. Transfection of adenovirus and treatments

The rAAV8 TBGp-SULT1E1-EGFP-3Flag-SV40 PolyA virus (0.1 mL per mouse) was administered via the tail vein of mice. Vehicle adeno-associated virus (AAV) was also administered via the tail vein (Mulorz et al., 2020). After 30 d, mice in the following groups were intragastrically administered the appropriate treatment for 30 d: the control and rAAV8-empty + con groups were administered 0.1 mL/10 g saline per day; the SPF, rAAV8-empty + SPF, and rAAV8-SULT1E1 + SPF groups were administered 10 g/kg SPF per day (Wu et al., 2022); the rAAV8-empty + psoralen and rAAV8-SULT1E1 + psoralen groups were administered 50 mg/kg psoralen per day; and the rAAV8-SULT1E1 + isopsoralen and rAAV8-empty + isopsoralen groups were administered 50 mg/kg isopsoralen per day. Blood was withdrawn from the postocular vein 24 h after the last SPF administration. Serum was obtained following centrifugation of blood at 1 508*g* for 15 min at 4 °C and stored at −80 °C before use. At the end of the experiments, mice were euthanized via cervical dislocation, and the livers were harvested between 9:00 am and 1:00 pm. A liver section was rapidly drenched in liquid nitrogen and then stored at −80 °C for subsequent experiments. The remaining liver segments were fixed in 10 % formalin for histopathological examination.

2.9. B-ultrasound examination in vivo

Mice were anesthetized via an intraperitoneal injection of 0.3 % pentobarbital sodium (0.1 mL/10 g). Thereafter, B-ultrasonography was performed to observe the lesions in the gallbladder and liver using Parkson (Model: Mylab Six, Italy).

2.10. Serum biochemistry

Serum samples were obtained from all animals via centrifugation of the blood samples at 3 302 r/min for 10 min at 4 °C (Microfuge 22R Centrifuge, Beckman, USA). The biochemistry of the serum samples was determined using an AU680 Beckman Coulter clinical chemistry analyzer.

2.11. ELISA

The levels of FXR, SULT1E1, and paraoxonase 1 (PON1) were determined using commercial ELISA kits (Jiancheng Bioengineering Institute, Nanjing, China) for each compound, according to the manufacturer's guidelines.

2.12. Histopathology

The liver, kidneys, spleen, and thymus were weighed. The liver was preserved in 4 % formalin or stored at −80 °C. Organ coefficients [(organ weight × 100)/body weight] were calculated. The organs and tissues were embedded in paraffin, sectioned, and stained with hematoxylin and eosin (H&E) and Hall's stain (liver).

2.13. Immunofluorescence examination

Some of the fresh liver tissue samples were stored at −80 °C. Thereafter, 7 mm-thick frozen sections were prepared and incubated with antibodies against Bsep (1:100, SAB Biotechnology), Mrp2 (1:100, SAB Biotechnology), and SULT1E1 (1:100, SAB Biotechnology) overnight at 4 °C using HistoCore Arcadia H Leica ASP embedding machine. The sections were then washed with phosphate-buffered saline and incubated with biotinylated anti-rat IgG/FITC antibodies (1:100, SAB Biotechnology) for 2 h at 37 °C. Images were captured using an Aperio Versa panoramic scanning system.

2.14. Western blot analysis

The liver proteins were collected using RIPA lysis buffer (Beyotime Biotechnology) containing 1 mmol/L phenylmethanesulfonyl fluoride and protease and phosphatase inhibitor cocktail (Yeasen). Protein concentrations were determined using a BCA kit (Beyotime Biotechnology). Equal amounts of protein samples (50 μg) were separated via SDS-PAGE and transferred onto a PVDF membrane (Millipore, Burlington, MA, USA). The membrane was blocked using non-fat dry milk (Bright Dairy and Food Co., Ltd, Shanghai, China) dissolved in Tris-buffered saline with Tween 20 (TBST) for 2 h and incubated overnight at 4 °C with the following antibodies:anti-FXR (1: 500, SANTA:L1719), anti-CYP7a1 (1: 500, SANTA:H1321), anti-Mrp2 (1: 1,000, SAB:29220), anti-Bsep (1: 1,000, SAB:29219), anti-HNF4α (1: 500, SANTA:H1820), anti-Nrf2 (1: 1,000, SAB:41255), anti-Ntcp (1: 1,000, SAB:29569), anti-IL-6 (1: 500, SANTA:sc-28343), anti-SULT1E1 (1: 1,000, SAB:29221), and anti-SULT2A1 (1: 1,000, SAB:G1917). The blots were washed and incubated with horseradish peroxidase-conjugated antibodies at 20–24 °C for 2 h. Finally, the membranes were washed three times with TBST and visualized using an enhanced chemiluminescence substrate (Immobilon ECL; Millipore).

2.15. Statistical analysis

All data were assessed using GraphPad Prism v.7 and are presented as mean ± standard deviation (SD). Significant differences between two groups were evaluated using Student's *t*-test. Multiple comparisons were performed using One-way analysis of variance (ANOVA). Differences with P values <0.05 were considered statistically significant.

3. Results

3.1. Multi-target liver damage induced by SPF

By employing the TCMSP, TCMID, and Batman-TCM databases, 45 components in SPF were analyzed, and 854 potential targets for drug-induced cholestasis were retrieved. By mapping the prediction targets of SPF with the drug-induced cholestasis-related targets, 151 potential common targets were obtained, which are displayed in the overlapping region in the Venn diagram and interactive network (Fig. 1A). The overlapping genes were then used to construct a PPI network using the STRING database (version 11.0). The PPI network contained 126 nodes and 733 edges. The average node degree was 9.71 (Fig. 1B). Topological analysis of the PPI network was carried out using the "Network Analyzer" function of Cytoscape, and the attributes of "betweenness centrality," "closeness centrality," and "topological coefficient" were retained. *EP300*, *TP53*, *JUN*, *ESR1*, *AKT1*, *RELA*, *SRC*, *STAT3*, *MAPK3*, *HDAC1*, and *MAPK1* were identified as the hub genes ranked by degree. A hub gene network was then generated. Based on the degree value of each compound or gene, we surmised the contribution of 42 compounds and 151 genes to the effect of SPF on drug-induced cholestasis. Based on PPI network enrichment results, psoralen, isopsoralen, neobavaisoflavone, bavachin, corylin, psoralidin, bavachinin, and corylifol A, 4′-*O*-methylbavachalcone were identified as the main compounds of the liver damage targets of SPF. ESR1 is one of the crucial target genes of liver damage induced by SPF. A total of 126 pathways were obtained via KEGG pathway enrichment analysis. The top 20 pathways included "PI3K-Akt", "lipid metabolism", "estrogen signaling", "TNF signaling", and "bile acid transport signaling", suggesting that the BA transport signaling and female excitation-related pathways are closely related to psoralea-induced liver damage (Fig. 1C and D).

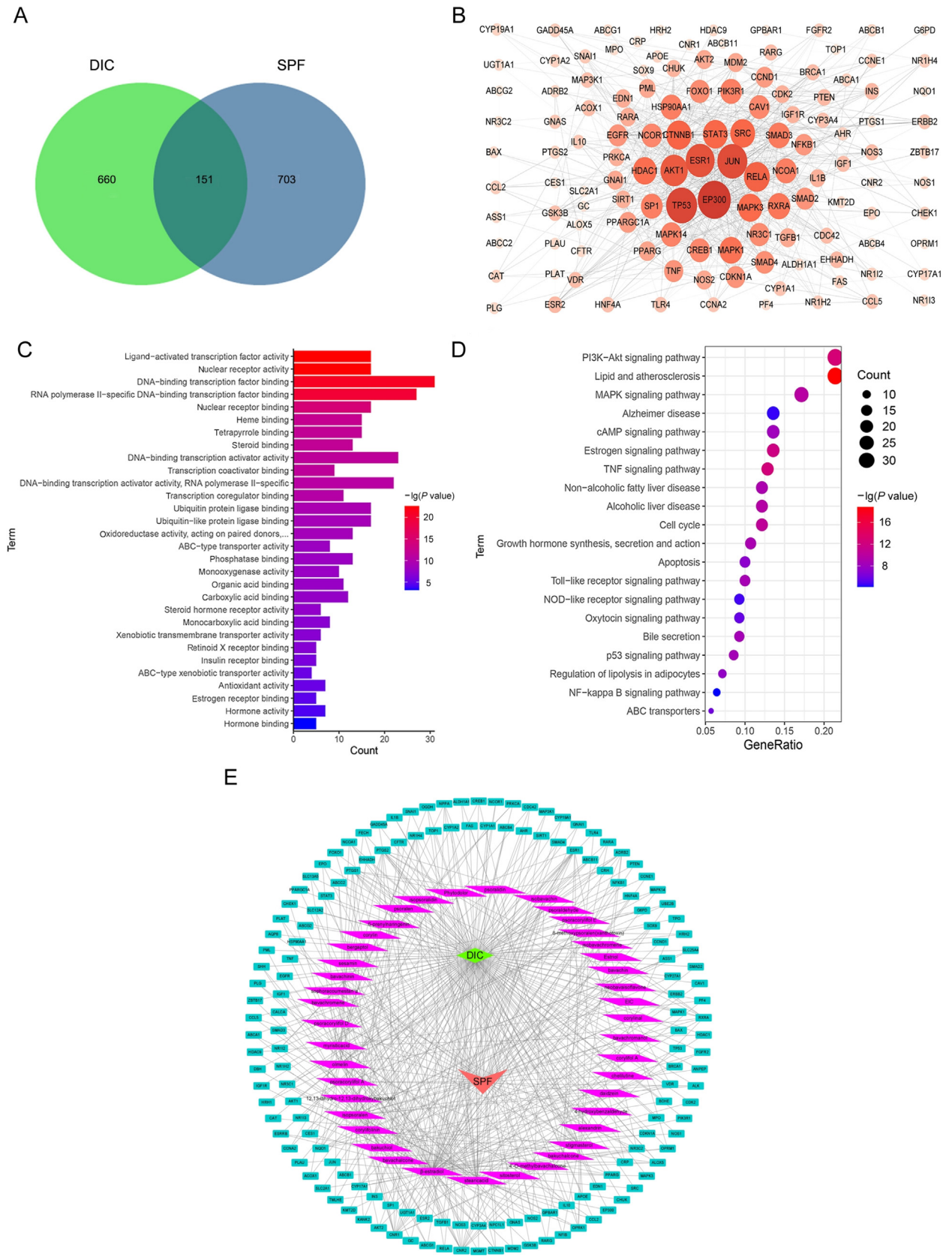

Fig. 1. Target prediction of SPF, network construction, and GO and KEGG enrichment analyses. (A) Venn diagram of the potential disease targets and SPF targets; the overlapping region contains 151 targets (DIC: Drug induced liver injury). (B) Protein-protein interaction (PPI) network. The larger the target and the darker the color, the larger the degree value. Among them, ESR1 represents the estrogen target with a degree value of 0.987, which is second only to EP300, TP53 and JUN.(C) GO enrichment analysis indicating the 188 overlapping targets. (D) KEGG enrichment analysis indicating the top 20 pathways. (E) Network construction of compounds, targets, and disease. The darker the color and the larger the node, the higher the degree.

3.2. HPLC fingerprint of SPF

We used an external standard method to calculate the concentrations of 10 components in the SPF decoction using references (Fig. 2, Table 1). According to the composition fingerprint, the concentrations of psoralenoside, isopsoralenoside, psoralen, isopsoralen, neobavaisoflavone, bavachin, isobavachalcone, bavachinin, corylifol A, and bakuchiol were determined [psoralenoside, (11.86 ± 0.46) mg/g; isopsoralenoside, (21.17 ± 0.86) mg/g; psoralen, (0.60 ± 0.04) mg/g; isopsoralen, (0.44 ± 0.03) mg/g; neobavaisoflavone (0.30 ± 0.04) mg/g; bavachin, (0.23 ± 0.05) mg/g; isobavachalcone, (0.13 ± 0.06) mg/g; bavachinin, (0.25 ± 0.03) mg/g ; corylifol A, (0.12 ± 0.02) mg/g; bakuchiol, (2.14 ± 0.66) mg/g].

3.3. Overexpression of SULT1E1 can improve gallbladder enlargement and gallbladder wall thickening

According to the B-ultrasound scan, the gallbladder size increased in the SPF, rAAV8-empty + SPF, rAAV8-empty + psoralen, and rAAV8-empty + isopsoralen groups compared to that in the control group, and the gallbladder wall thickened to varying degrees (Fig. 3). Gallbladder enlargement was more evident in the SPF, rAAV8-empty + SPF, and rAAV8-empty + isopsoralen groups, with average gallbladder sizes of 5.0 mm, 4.9 mm, and 5.7 mm, respectively. Of note, the average gallbladder size of the control and rAAV8-empty + con groups was only 4.1 mm. SULT1E1 overexpression reduced the enlarged gallbladder size and the thickness of the gallbladder wall [rAAV8-empty + SPF *vs* rAAV8-SULT1E1 + SPF: mean gallbladder size, (4.90 ± 0.61) mm *vs* (4.30 ± 0.45) mm; rAAV8-empty + psoralen *vs* rAAV8-SULT1E1 + psoralen: mean gallbladder wall thickness, (0.49 ± 0.07) mm *vs* (0.38 ± 0.05) mm; and rAAV8-empty + isopsoralen *vs* rAAV8-SULT1E1 + isopsoralen: mean gallbladder size, (5.60 ± 0.41) mm *vs* (4.90 ± 0.55) mm]. Isopsoralen-induced cholestasis and gall bladder enlargement were most notable in the *in vivo* B-ultrasound scan images.

3.4. Overexpression of SULT1E1 improves liver damage index

The six most used biomarkers for the diagnosis and assessment of hepatic diseases in clinical medicine, namely ALT, AST, and ALP activities, and TBIL, IBIL, and TBA levels, were evaluated; the results are summarized in Fig. 4. The values for the six indices in the control group and rAAV8-empty + con group were similar, with no significant difference found. Such finding indicates that vehicle AAV8 did not exhibit adverse effects. Following the administration of SPF, psoralen, and isopsoralen, the six biochemical indices of liver damage increased to varying degrees. In fact, the SPF, rAAV8-empty + SPF, rAAV8-empty + psoralen, and rAAV8-empty + isopsoralen groups exhibited significant increases in the liver biochemical indices [AST: rAAV8-empty + con *vs* SPF, rAAV8-empty + SPF, rAAV8-empty + psoralen, rAAV8-empty + isopsoralen: (141.50 ± 9.30) U/L *vs* (184.28 ± 15.42) U/L, (180.72 ± 9.92) U/L, (157.21 ± 10.12) U/L, (185.78 ± 10.00) U/L]. Moreover, ALP, ALT, AST, TBIL, IBIL, and TBA levels in the SULT1E1-overexpressed AAV8 groups were significantly different from those in the corresponding vehicle AAV8 groups. Therefore, SULT1E1 overexpression could improve cholestatic liver damage induced by SPF, psoralen, and isopsoralen [such as AST: rAAV8-empty + SPF *vs* rAAV8-SULT1E1 + SPF, (180.72 ± 9.92) U/L *vs* (152.21 ± 14.82) U/L; rAAV8-empty + psoralen *vs* rAAV8-SULT1E1 + psoralen: (157.21 ± 10.12) U/L *vs* (146.80 ± 12.77) U/L]. Moreover, isopsoralen rather than psoralen may cause cholestasis, as shown in Table 2.

3.5. Overexpression of SULT1E1 improves organ coefficients

Compared to the coefficients in the rAAV8-empty + con group, the organ coefficients of the liver significantly increased in the other groups, except the rAAV8-SULT1E1 + psoralen and rAAV8-SULT1E1 + SPF groups (Table 3). Hepatic enlargement was most notable in the rAAV8-empty + isopsoralen group [rAAV8-empty + con *vs* rAAV8-empty + isopsoralen: (32.52 ± 3.28) mg/g *vs* (41.38 ± 3.91) mg/g, $^{***}P < 0.001$]. Similar to the biochemical analyses, the values obtained for the SULT1E1-overexpressed AAV8 groups were significantly different from those obtained for the corresponding vehicle AAV8 groups [$^{\#}P < 0.05$, rAAV8-empty + SPF *vs* rAAV8-SULT1E1 + SPF, (40.84 ± 3.82) mg/g *vs* (37.32 ± 1.85) mg/g; rAAV8-empty + isopsoralen *vs* rAAV8-SULT1E1 + isopsoralen: (41.38 ± 3.91) mg/g *vs* (37.24 ± 1.97) mg/g]. Based on this result, SULT1E1 overexpression can improve hepatomegaly induced by SPF, psoralen, and isopsoralen. The organ coefficients of the ovarian indices increased in the SPF and rAAV8-empty + SPF groups compared to those in the rAAV8-empty + con group; however, the organ coefficients decreased in the rAAV8-empty + psoralen and rAAV8-empty + isopsoralen groups compared to those in the rAAV8-empty + con group [(0.93 ± 0.08) mg/g, (0.91 ± 0.10) mg/g *vs* (0.71 ± 0.10) mg/g; (0.58 ± 0.09) mg/g, (0.53 ± 0.05) mg/g *vs* (0.71 ± 0.10) mg/g]. Such findings indicate that SULT1E1 overexpression can either increase or decrease the ovarian index, thereby restoring the normal value.

3.6. Overexpression of SULT1E1 improves liver damage and levels of estrogen-related markers

FXR maintains BA homeostasis and is one of the most important sensors of BA levels. The FXR expression levels significantly decreased in all rAAV8-empty groups (rAAV8-empty + SPF, rAAV8-empty + psoralen, rAAV8-empty + isopsoralen) and the SPF group compared with that in the control group. SULT1E1 overexpression could increase FXR levels; however, these levels were decreased after treatment with SPF and isopsoralen [rAAV8-empty + SPF *vs* rAAV8-SULT1E1 + SPF: (830.74 ± 43.04) pg/mg *vs* (990.10 ± 49.54) pg/mg]; rAAV8-empty + isopsoralen *vs* rAAV8-SULT1E1 + isopsoralen: (831.64 ± 88.52) pg/mg *vs* (1 210.19 ± 51.21) pg/mg]. Serum SULT1E1 level was found to decrease after 30 d of intragastric SPF administration [rAAV8-empty + con *vs* SPF, (12.97 ± 0.88) ng/mg *vs* (8.76 ± 0.98) ng/mg $^{*}P < 0.05$; rAAV8-empty + con *vs* rAAV8-empty + SPF, (12.97 ± 0.88) ng/mg *vs* (8.28 ± 1.20) ng/mg, $^{**}P < 0.01$]. However, SULT1E1-overexpressed AAV effectively elevated the decreased level of SULT1E1 [AAV8-empty + psoralen *vs* rAAV8-SULT1E1 + psoralen: (9.65 ± 0.93) ng/mg *vs* (12.93 ± 0.56) ng/mg, $^{\#\#}P < 0.01$; AAV8-empty + isopsoralen *vs* rAAV8-SULT1E1 + isopsoralen: (9.26 ± 1.02) ng/mg *vs* (12.33 ± 1.42) ng/mg, $^{\#}P < 0.05$]. Compared to the levels in the AAV8-empty + con group, PON1 levels significantly decreased in the SPF and rAAV8-empty + SPF groups [$^{*}P < 0.05$, PON1 levels: rAAV8-empty + con *vs* SPF and rAAV8-empty + SPF, (8.40 ± 1.09) ng/mg *vs* (5.25 ± 0.30) ng/mg and (5.40 ± 0.97) ng/mg]. These results were shown in Fig. 5A.

3.7. Overexpression of SULT1E1 improves pathological liver damage

Histopathology revealed edema with varying degrees of inflammatory infiltrates in the rAAV8-empty groups (rAAV8-empty + SPF, rAAV8-empty + psoralen, rAAV8-empty + iopsoralen) (Fig. 5B). In the SPF group, liver cells had slight vacuolation degeneration and liver cord disorder. Sinus gap widening was also evident in this group. Notably, part of the liver cord appeared long and thin. The

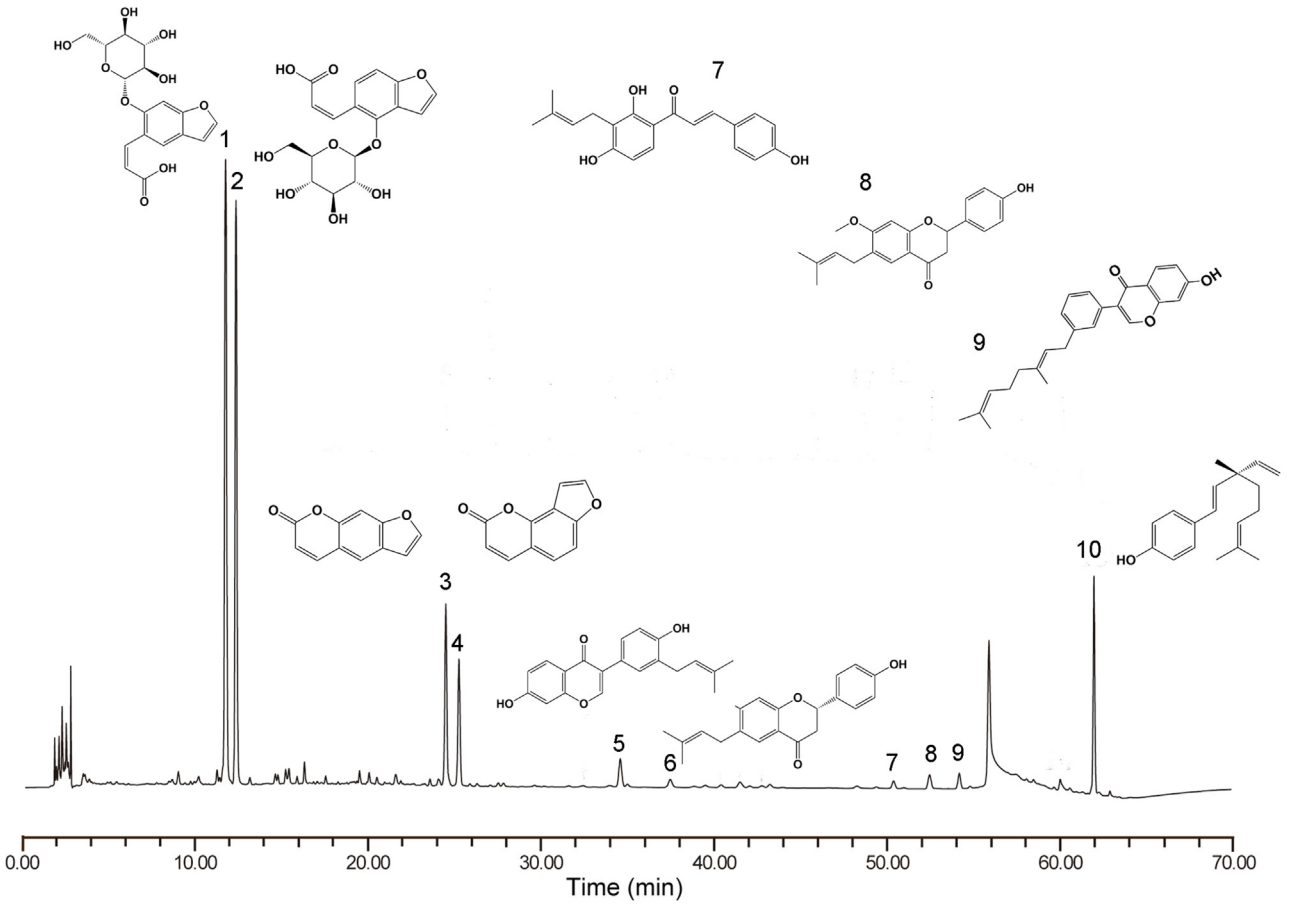

Fig. 2. Fingerprint of the SPF decoction (n = 3). (1) Psoralenoside; (2) Isopsoralenoside; (3) Psoralen; (4) Isopsoralen; (5) Neobavaisoflavone; (6) Bavachin; (7) Isobavachalcone; (8) Bavachinin; (9) Corylifol A and (10) Bakuchiol.

Table 1
Composition analysis of *Psoraleae Fructus* decoction.

Compositions	Concentration (mg/g)
Psoralenside	11.86 ± 0.46
Isopsoralenoside	21.17 ± 0.86
Psoralen	0.60 ± 0.04
Isopsoralen	0.44 ± 0.03
Neobavaisoflavone	0.30 ± 0.04
Bavachin	0.23 ± 0.05
Isobavachalcone	0.13 ± 0.06
Bavachinin	0.25 ± 0.03
Corylifol A	0.12 ± 0.02
Bakuchiol	2.14 ± 0.66

Note: quantifiable eight components.

rAAV8-empty + SPF group displayed the same phenomenon and exhibited inflammatory cell infiltration. After injecting SULT1E1-overexpressed AAV into the tail vein, the pathological sections of liver lesions were clear, with only local microvacuolar degeneration observed. Other evidence of damage was not observed. Both the rAAV8-empty + psoralen and rAAV8-empty + isopsoralen groups displayed partial hepatic cell vacuolation degeneration, sporadic hepatic cell nucleus shrinkage, hepatic cord disorder, and some inflammatory cell infiltration. The corresponding groups administered SULT1E1-overexpressed AAV had reduced liver damage.

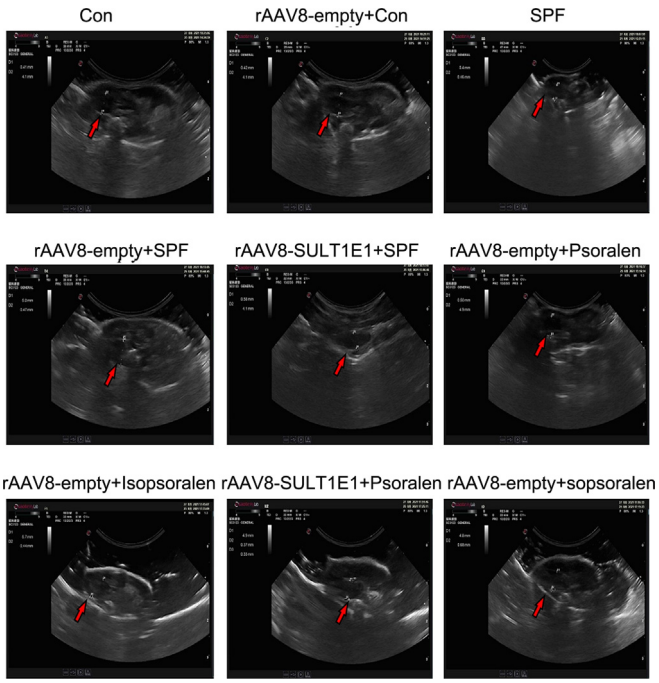

Fig. 3. *In vivo* B-ultrasound images of mice. Overexpression of SULT1E1 can improve gallbladder enlargement and gallbladder wall thickening. The red arrow indicates the gallbladder.

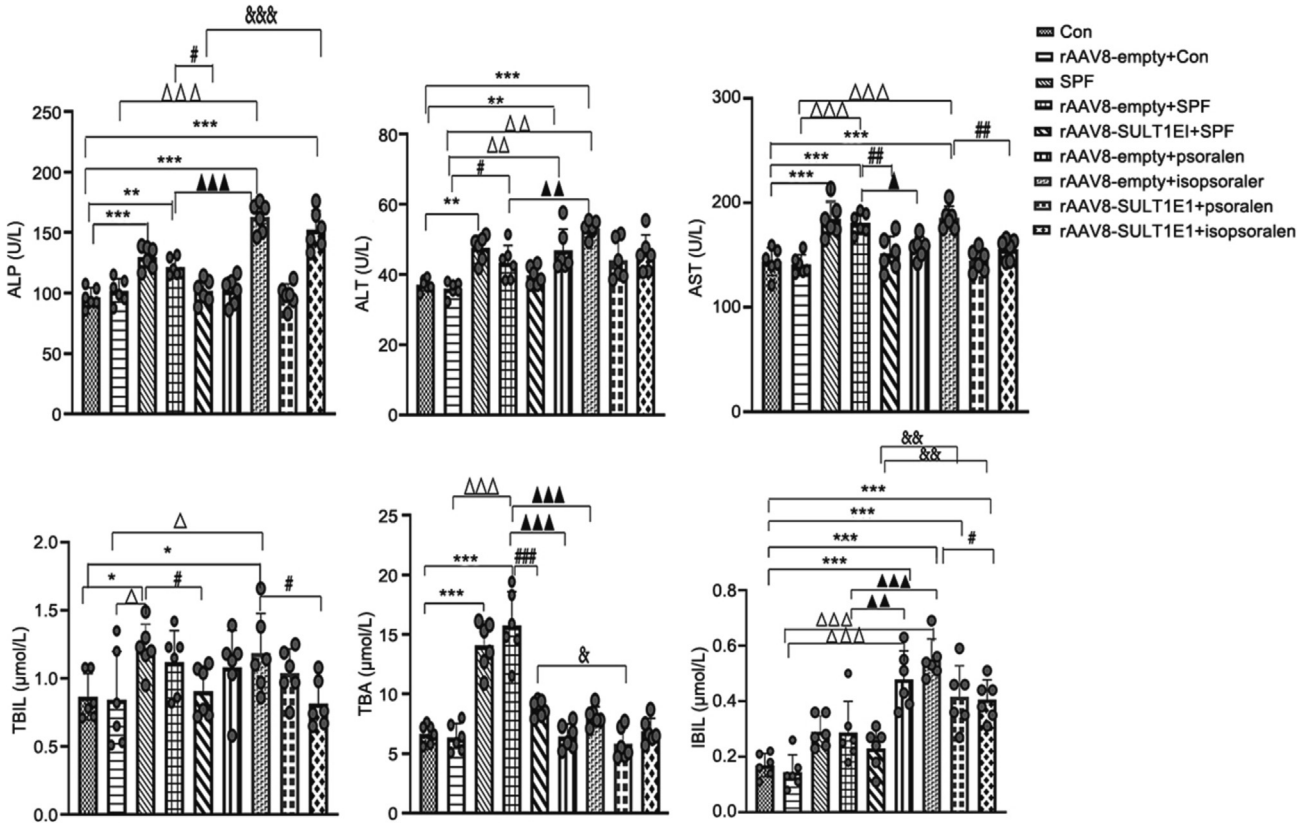

Fig. 4. Levels of serum biochemical parameters. The data are expressed as mean ± SD (n = 6). Significant differences relative to the data from the control group ($^{*}P < 0.05$, $^{**}P < 0.01$, $^{***}P < 0.001$); rAAV8-empty + con group ($^{\triangle}P < 0.05$, $^{\triangle\triangle}P < 0.01$, $^{\triangle\triangle\triangle}P < 0.001$); rAAV8-empty + SPF group ($^{\blacktriangle}P < 0.05$, $^{\blacktriangle\blacktriangle}P < 0.01$, $^{\blacktriangle\blacktriangle\blacktriangle}P < 0.001$); and rAAV8-SULT1E1 + SPF group ($^{\&}P < 0.05$, $^{\&\&}P < 0.01$, $^{\&\&\&}P < 0.001$). Comparison of the rAAV8-empty and rAAV8-SULT1E1 groups to their corresponding treatment group ($^{\#}P < 0.05$, $^{\#\#}P < 0.01$, $^{\#\#\#}P < 0.001$).

Table 2
Biochemical indexes of liver damage (mean ± SD, n = 6).

Groups	ALP (U/L)	ALT (U/L)	AST (U/L)	TBIL (μmol/L)	TBA (μmol/L)	IBIL (μmol/L)
Con	96.27 ± 7.41	36.69 ± 1.90	143.6 ± 12.16	0.87 ± 0.16	6.83 ± 0.86	0.17 ± 0.04
SPF	128.51 ± 8.78	46.19 ± 4.86	184.28 ± 15.42	1.12 ± 0.31	14.12 ± 1.88	0.28 ± 0.05
rAVV8-empty + Con	101.49 ± 9.23	35.35 ± 2.40	141.51 ± 9.30	0.88 ± 0.34	6.51 ± 1.14	0.16 ± 0.07
rAVV8-empty + SPF	121.28 ± 7.32	43.41 ± 4.88	180.72 ± 9.92	1.12 ± 0.23	15.74 ± 2.84	0.29 ± 0.11
rAVV8-SULT1E1 + SPF	100.61 ± 9.24	39.02 ± 2.63	152.22 ± 14.82	0.91 ± 0.16	9.00 ± 0.70	0.23 ± 0.07
rAVV8-empty + psoralen	101.92 ± 11.37	46.80 ± 6.11	157.22 ± 10.12	1.08 ± 0.27	6.45 ± 1.05	0.48 ± 0.10
rAVV8-empty + isopsoralen	163.29 ± 11.15	51.62 ± 4.54	185.79 ± 9.99	1.13 ± 0.31	8.19 ± 0.73	0.55 ± 0.07
rAVV8-SULT1E1 + psoralen	98.30 ± 8.09	44.04 ± 4.86	146.80 ± 12.77	1.07 ± 0.17	5.59 ± 1.20	0.40 ± 0.13
rAVV8-SULT1E1 + isopsoralen	152.80 ± 14.67	46.00 ± 4.90	159.06 ± 12.02	0.85 ± 0.19	6.87 ± 0.97	0.41 ± 0.10

Table 3
Effects of SPF on organ coefficients (mean ± SD).

Groups	Liver index (mg/g)	Spleen index (mg/g)	Renal index (mg/g)	Ovarian index (mg/g)
Con	32.73 ± 2.59	3.64 ± 0.32	11.16 ± 0.65	0.73 ± 0.05
rAAV8-empty + Con	32.52 ± 3.28	3.59 ± 0.42	11.18 ± 1.42	0.71 ± 0.10
SPF	40.98 ± 2.14***	3.60 ± 0.21	11.14 ± 0.79	0.93 ± 0.08*
rAAV8-empty + SPF	40.84 ± 3.82***	3.66 ± 0.26	10.94 ± 0.40	0.91 ± 0.10*
rAAV8-SULT1E1 + SPF	37.32 ± 1.85$^{\#}$	3.61 ± 0.19	10.55 ± 0.34	0.72 ± 0.17$^{\#}$
rAAV8-empty + psoralen	39.66 ± 1.05**	3.36 ± 0.28	11.21 ± 0.66	0.58 ± 0.09*
rAAV8-empty + isopsoralen	41.38 ± 3.91***	3.37 ± 0.31	11.41 ± 0.42	0.53 ± 0.05*
rAAV8-SULT1E1 + psoralen	37.74 ± 2.32$^{\#}$	3.57 ± 0.18	11.90 ± 0.49	0.72 ± 0.08$^{\#}$
rAAV8-SULT1E1 + isopsoralen	37.24 ± 1.97$^{\#*}$	3.68 ± 0.31	11.88 ± 0.82	0.65 ± 0.09

$^{*}P < 0.05$, $^{**}P < 0.01$, $^{***}P < 0.001$ compared with the rAAV8-empty+Con group; $^{\#}P < 0.05$, $^{\#\#}P < 0.01$ comparisons between SULT1E1 overexpression group and corresponding vehicle adeno-associated virus.

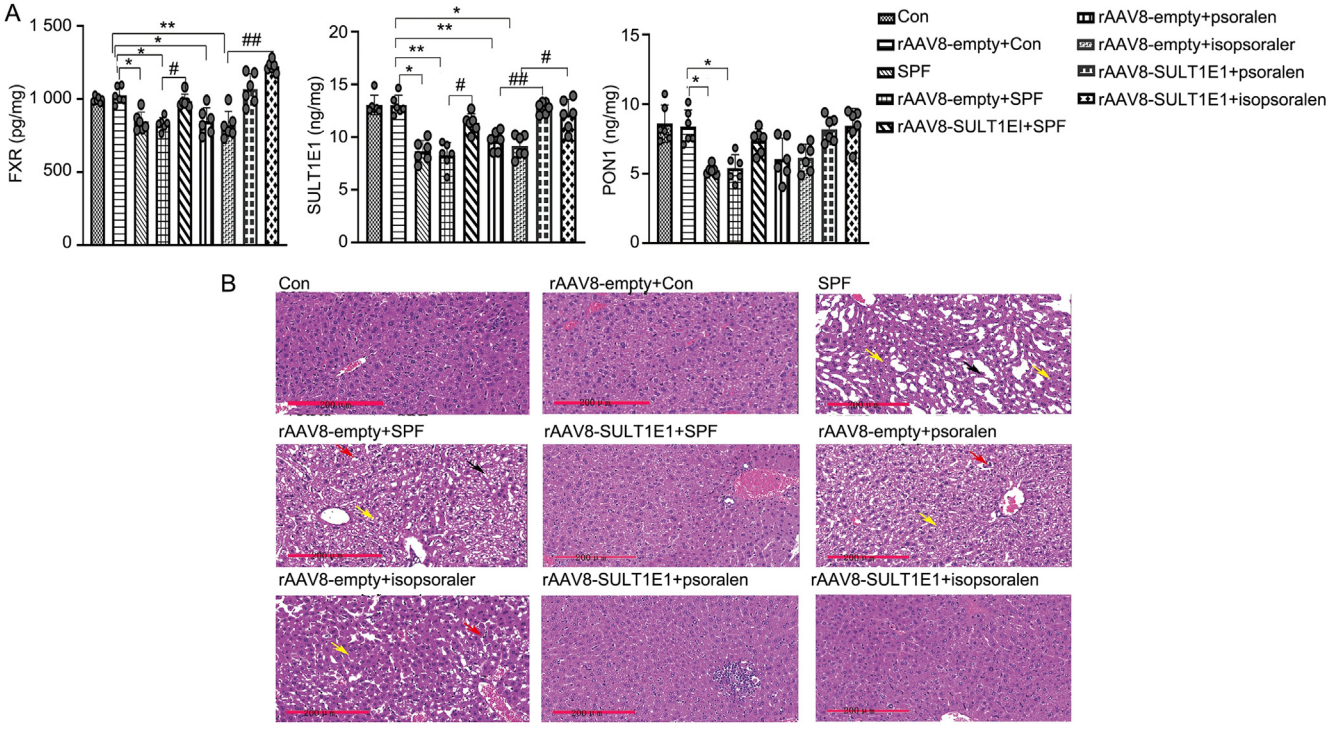

Fig. 5. (A) Serum levels of FXR, SULT1E1, and PON1 based on ELISA. The data are expressed as mean ± SD (n = 6). Significant differences relative to the data from the rAAV8-empty + con group ($^{*}P < 0.05$, $^{**}P < 0.01$, $^{***}P < 0.001$). Comparisons of the rAAV8-empty and rAAV8-SULT1E1 groups to their corresponding treatment group ($^{\#}P < 0.05$, $^{\#\#}P < 0.01$, $^{\#\#\#}P < 0.001$). (B) Histopathologic evaluation (H & E staining) of the liver tissues (black arrows indicate hepatic cord disorders; yellow arrows indicate hepatic vacuolar degeneration; red arrows indicate inflammatory infiltration; n = 6).

3.8. Overexpression of SULT1E1 increases fluorescence intensity of Bsep and Mrp2

To further confirm the role of SULT1E1 in SPF-induced cholestatic liver damage, immunofluorescence staining of Bsep and Mrp2 in the liver was performed. The livers of mice in the SPF, rAAV8-empty + SPF, rAAV8-empty + psoralen, and rAAV8-empty + isopsoralen groups had a notable decrease in the levels of Bsep and Mrp2 compared to those of mice in the rAAV8-empty + con group. Further, the levels of SULT1E1 were notably increased in the livers of the rAAV8-SULT1E1 groups. The positive expression rate of Mrp2 and Bsep in the SULT1E1-overexpressed groups was higher than that in the corresponding vehicle AAV8 groups. These results were shown in Fig. 6 and Table 4.

3.9. Overexpression of SULT1E1 improves levels of FXR-SULT1E1 signaling pathway indicators

Of the groups administered the SULT1E1-overexpressed AAV, SULT1E1 was demonstrated to be overexpressed in the rAAV8-SULT1E1 groups (Fig. 7A). To investigate the mechanism underlying SPF-induced hepatotoxicity and cholestasis, we focused on the hepatic nuclear receptor, FXR, and the estrogen-inactivating enzyme, SULT1E1, which are closely related to BA homeostasis. Compared to rAAV8-empty + con, the expression level of FXR decreased in the rAAV8-empty + SPF group and tended to increase in the rAAV8-SULT1E1 + SPF group compared with the rAAV8-empty + SPF group. A more evident decrease in the expression level of FXR was found in the isopsoralen group relative to that in the psoralen group. SULT1E1 overexpression could alleviate the SPF-, psoralen-, and isopsoralen-induced decrease in FXR expression. Furthermore, the expression of hepatocyte nuclear factor 4 alpha (HNF4α), which plays a critical role in the FXR-SULT1E1 signaling pathways, was determined. SULT1E1 overexpression could alleviate the SPF-induced decrease in HNF4α expression. The expression level of the synthesis-related enzyme, CYP7a1, increased, whereas that of the metabolism-related enzyme, SULT2A1, decreased in the SPF, psoralen, and isopsoralen groups. When SULT1E1-overexpressed AAV8 was administered via the tail vein of mice, the increased levels of CYP7a1, which were originally elevated after drug administration, decreased compared to those in the control group. Further, the decreased levels of SULT2A1, which were originally reduced after drug administration, increased compared to those in the control group. In the rAAV8-empty + SPF, rAAV8-empty + psoralen, and rAAV8-empty + isopsoralen groups, the expression levels of the efflux transporters, Bsep and Mrp2, were significantly decreased compared with those in the rAAV8-empty + con group. The declining trend of Bsep and Mrp2 was more evident in the isopsoralen group relative to the psoralen group. Notably, this declining trend was reversed upon overexpression of SULT1E1. The uptake of the transporter, Ntcp, also decreased in the SPF-, psoralen-, and isopsoralen-treated groups, and the declining trend was reversed upon overexpression of SULT1E1. Nrf2 is an essential transcription factor that regulates the expression of several detoxifying and antioxidant defense genes in the liver. The Nrf2 expression levels were found to decrease in the SPF and rAAV8-empty + SPF groups. Compared to the levels in the rAAV8-empty + con group, the Nrf2 expression levels significantly decreased in the rAAV8-empty + isopsoralen group compared with those in the rAAV8-empty + psoralen group. The declining trend was reversed upon overexpression of SULT1E1. Such finding indicates that liver detoxification functions are suppressed following SPF, psoralen, and isopsoralen treatment and overexpression of SULT1E1 can improve the levels of the detoxifying and antioxidant defense gene, *Nrf2*. SULT1E1 expression significantly decreased in the rAAV8-empty + SPF, rAAV8-empty + psoralen, and rAAV8-empty + isopsoralen groups. Further, the expression levels of SULT1E1 and HNF4α were significantly

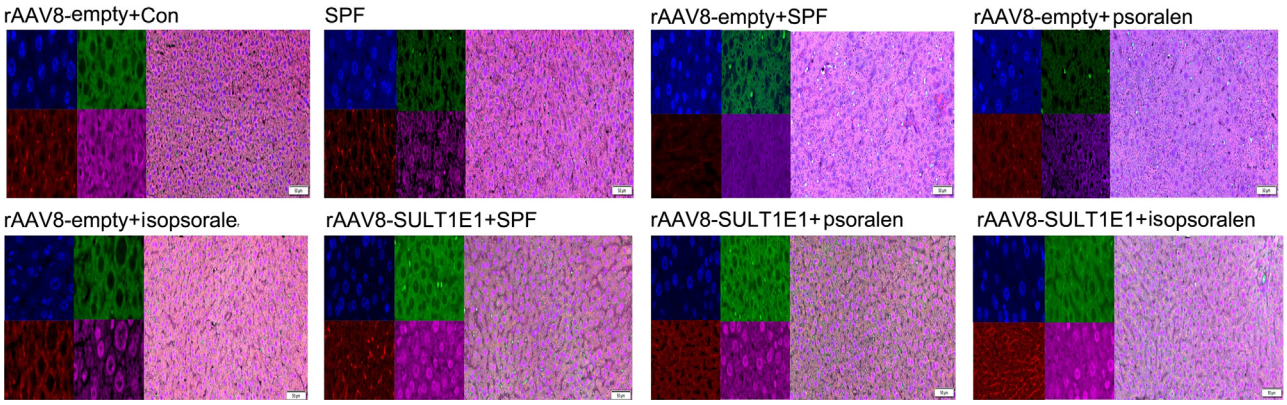

Fig. 6. Trichromatic immunofluorescence analysis. Green fluorescence indicates EGFP; red fluorescence indicates Bsep; and magenta fluorescence indicates Mrp2.

Table 4
Analysis of dual immunofluorescence (mean ± SD).

Groups	Bsep (Positive rate/%)	Mrp2 (Positive rate/%)	Bsep & Mrp2 (Positive rate/%)
rAAV8-empty + Con	78.22 ± 10.28	63.93 ± 8.42	55.60 ± 9.42
SPF	25.14 ± 6.34***	16.89 ± 3.21***	14.14 ± 3.79***
rAAV8-empty + SPF	25.13 ± 5.82***	17.73 ± 4.26***	15.16 ± 4.40***
rAAV8-empty + psoralen	23.94 ± 4.35***	26.24 ± 4.68***	18.21 ± 3.56***
rAAV8-empty + isopsoralen	27.96 ± 6.91***	22.31 ± 6.71***	14.41 ± 4.67***
rAAV8-SULT1E1 + SPF	48.57 ± 8.55$^{\#\#\#***}$	41.76 ± 7.57$^{\#\#\#*}$	36.37 ± 6.38$^{\#\#**}$
rAAV8-SULT1E1 + psoralen	39.29 ± 6.32$^{\#***}$	41.36 ± 7.18$^{\#*}$	29.37 ± 5.49$^{\#\#**}$
rAAV8-SULT1E1 + isopsoralen	31.38 ± 5.97***	29.30 ± 5.31**	20.85 ± 3.82$^{\#***}$

$^{*}P < 0.05$, $^{**}P < 0.01$, $^{***}P < 0.001$ compared with the rAAV8-empty+Con group; $^{\#}P < 0.05$, $^{\#\#}P < 0.01$ comparisons between SULT1E1 overexpression group and corresponding vehicle adeno-associated virus.

decreased in the rAAV8-empty + SPF groups. Of note, HNF4α expression did not change in the psoralen and isopsoralen groups (Fig. 7B).

4. Discussion

Psoralea corylifolia L. was first recorded in *Kaibao Materia Medicina*. *P. corylifolia* tonifies the kidneys and strengthens the Yang, thereby consolidating essence, suppressing enuresis, warming the spleen, and preventing diarrhea. *P. corylifolia* is primarily used as a tonic (Zhang et al., 2024). However, due to improper clinical use or misuse, resulting in liver damage. Long-term heavy use may cause liver damage to a certain extent. The hepatotoxicity of SPF is one of the primary factors restricting its wider use. According to previous experiments, SPF hepatotoxicity is closely related to the FXR/SULT1E1 signaling pathway (Wu et al., 2022).

The hepatotoxicity of SPF is one of the primary factors restricting its wider use. A total of 45 components in SPF were analyzed, and 854 potential targets for drug-induced cholestasis were retrieved. *EP300*, *TP53*, *JUN*, *ESR1*, *AKT1*, *RELA*, *SRC*, *STAT3*, *MAPK3*, *HDAC1*, and *MAPK1* were identified as hub genes, and 151 genes were speculated to contribute to the effect of SPF in drug-induced cholestasis. Based on the PPI network enrichment results, psoralen, isopsoralen, neobavaisoflavone, bavachin, corylin, psoralidin, bavachinin, corylifol A, and 4′-*O*-methylbavachalcone were identified as the main compounds of SPF-induced liver damage. ESR1 is one of the target genes with high correlation, indicating that ESR1 has a crucial role in liver damage induced by SPF. Psoralen, isopsoralen, and other components in SPF exhibit phytoestrogenic effects and can activate ESR1 and ESR2. A total of 126 pathways were obtained using KEGG pathway enrichment analysis, with the "estrogen signaling pathway" and "bile acid transport" identified among the top 20 signaling pathways. Of note, the PI3K/Akt signaling pathway ranked first, MAPK signaling pathway ranked third, and estrogen signaling pathway ranked fifth. All three pathways are involved in estrogen signal transduction, and the estrogen pathway is directly related to estrogen. Therefore, the estrogen signaling pathway might be an important mechanism of psoraleae-induced liver damage.

The AST, ALP, ALT, TBIL, TBA, and IBIL activities were significantly higher in the rAAV8-drug treated group than in the rAAV8-empty group. The AST, ALP, ALT, TBIL, TBA, and IBIL activities were significantly higher than those in the rAAV8-empty group. These indices were higher in the rAAV8-empty + iso psoralen group than in the rAAV8-empty + psoralen and rAAV8-empty + SPF groups, suggesting that liver damage may be severe in isopsoralen group. These results are consistent with those of previous studies, in which the administration of psoralen and isopsoralen was found to repress the expression of CYP7a1, Bsep, Mrp2, and SULT2A1, and increase the expression of FXR and MRP3 in rat livers (Bi et al., 2015). Isopsoralen is reported to be more toxic than psoralen (Wang et al., 2019). Decreased serum levels of PON1 serve as an early indicator of liver damage. This measurement is more sensitive than the determination of the AST and ALT activities (Soliman, Karam, Mekkawy, & Ghorab, 2020). FXR regulates BA homeostasis and is an important factor in the pathogenesis of cholestasis (Herraez et al., 2012). FXR can upregulate BSEP and Mrp2 and repress the expression of Ntcp, CYP7a1, and CYP8b1 (Meng et al., 2015; Song et al., 2014; Bechmann et al., 2013). Following ligand activation, FXR promotes BA secretion by inducing the expression of efflux transporters, such as Bsep and Mrp2. FXR also reduces BA reabsorption by decreasing the expression of uptake transporters, such as Ntcp and sodium-independent organic anion transporters (OATPs) (Halilbasic, Claudel, & Trauner, 2013). FXR suppresses the expression of CYP7a1 and CYP8b1, reducing BA synthesis and inducing the expression of

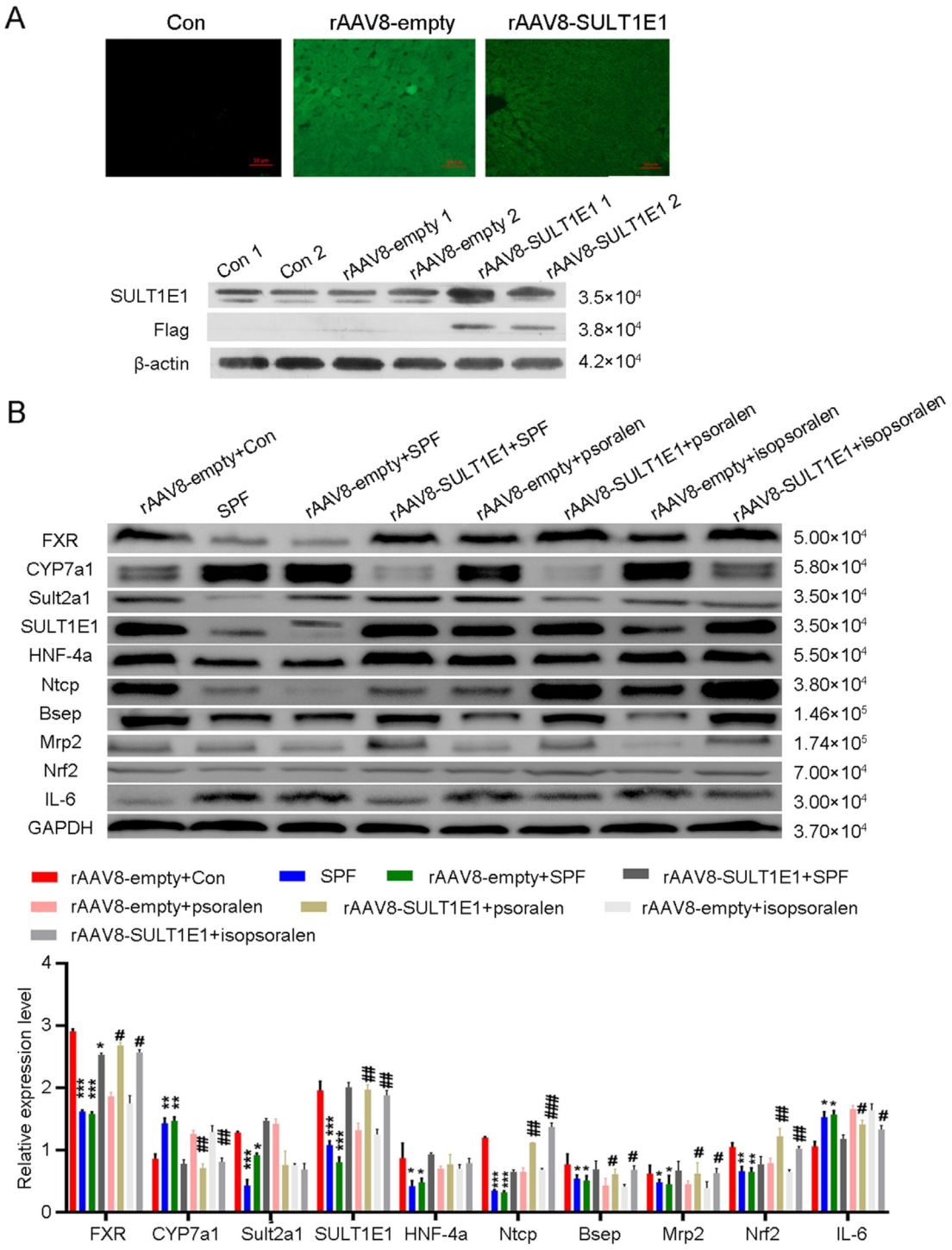

Fig. 7. (A) Successful construction of the SULT1E1 overexpression model. (B) Western blotting revealed the protein expression levels of FXR, Mrp2, CYP7a1, Bsep, Ntcp, Nrf2, Sult2a1, IL-6, HNF4α, and SULT1E1 in the liver. Specific band intensities were quantified and normalized to that of GAPDH (internal control). The data are presented as mean ± SD (n = 3). $^{*}P < 0.05$, $^{**}P < 0.01$, $^{***}P < 0.001$ *vs* the rAAV8-empty + Con group; $^{\#}P < 0.05$, $^{\#\#}P < 0.01$, $^{\#\#\#}P < 0.001$ *vs* the corresponding rAAV8-empty and rAAV8-SULT1E1 groups.

CYP3A2 and SULT1E1 to promote BA detoxification (Chiang, 2013). The expression levels of PON1 and FXR significantly decreased in mice in the SPF-, psoralen-, and isopsoralen-treated groups. Notably, the decreases in PON1 and FXR were reversed upon overexpression of SULT1E1.

The liver is the primary site of estrogen metabolism. SULT1E1 has long been recognized as a phase II metabolizing enzyme that primarily sulfonates and deactivates estrogens (Barbosa, Feng, Yu, Huang, & Xie, 2019). The estrogen sulfotransferase, SULT1E1, sulfates and inactivates estrogen, which is reactivated via desulfation by steroid sulfatase, thereby regulating estrogen homeostasis (Fashe, Hashiguchi, Yi, Moore, & Negishi, 2018). The plasma deoxycholic acid levels were 52 % higher in postmenopausal patients with breast cancer than in healthy controls (Costarelli & Sanders, 2002). This result supports the concept of a correlation between BA-associated disorders and estrogen-related diseases. Estrogen-

induced cholestasis is characterized by the impairment of BA uptake and secretion, which results in the accumulation of toxic BAs and alteration of BA composition, subsequently leading to liver damage (Marrone et al., 2016). Immunofluorescence analysis revealed that the positive fluorescence rate of Mrp2 and Bsep was higher in the SULT1E1-overexpressed AAV groups than that in the rAAV8-empty groups. To further determine the key role of SULT1E1, western blot was performed to determine the expression levels of FXR, Bsep, Mrp2, Sult2a1, CYP7a1, Ntcp, Nrf2, HNF4α, IL-6, and SULT1E1 in the liver samples. Based on our results, the expression levels of the uptake transporter, Ntcp, and the efflux transporters, Bsep and Mrp2, decreased. Notably, the decrease in the levels of efflux transporters was more pronounced. SPF inhibits the expression of CYP7a1, Bsep, and other bile transport-related proteins, and that of CYP450, resulting in cholestatic liver damage in rats (Wang et al., 2012). The expression levels of IL-6 increased in the rAAV8-drug treated group compared to that in the rAAV8-empty + con group. HNF4α is a liver-enriched master regulator of liver function. SULT1E1 regulation was abolished upon silencing of HNF4α (a known activator of SULT1E1). Rifampicin represses the transcription of SULT1E1 in hepatocytes via interactions with HNF4α (Kodama Kodama, Hosseinpour, Goldstein, & Negishi, 2011). FXR transcriptionally regulates the expression of SULT1E1 by inhibiting the binding of PGC1a to HNF4α (Wang, Yuan, Lu, Guo, & Wu, 2017). HNF4α regulates various genes to maintain liver function. In Hnf4α$^{\Delta Hep}$ mice, the expression levels of fatty acid oxidation-related genes, which are PPARα target genes, was increased compared to the decreased expression of PPARα. Such finding suggests that Hnf4α$^{\Delta Hep}$ mice take up more lipids than glucose in the liver. Furthermore, Hnf4α$^{\Delta Hep}$/Ppara$^{-/-}$ mice, which are deficient in both HNF4α and PPARα, exhibited improved hepatosteatosis and fibrosis (Kasano-Camones et al., 2023). The upstream factor, HNF4α, was found to decrease in the SPF and rAAV8-empty + SPF groups; however, when SULT1E1 was overexpressed, the HNF4α expression did not change significantly. Nrf2-mediated antioxidant genes are considered important components of the antioxidative defense mechanisms (Gao et al., 2013). Nrf2 was found to decrease in the groups treated with SPF, psoralen, and isopsoralen. Nrf2 exerts antioxidant effects and may be implicated in decreased lipid accumulation and attenuation of liver damage. The deletion of Nrf2 is reported to induce rapid progression of steatohepatitis in mice fed an atherogenic plus high-fat diet. Therefore, Nrf2 plays a crucial role in non-alcoholic fatty liver disease (Okada et al., 2013). Liver fibrosis is closely related to liver damage. Whether liver damage induced by SPF can cause liver fibrosis should be further discussed (Zhao et al., 2015).

According to previous experiments, SPF regulates the FXR-SULT1E signaling pathway through HNF4α, which is an important causative factor for cholestasis. The SULT1E1-overexpressed AAV was constructed and compared with the negative control, rAAV8-empty + con. Based on our findings, SULT1E1 was identified as an important target of the cholestatic liver damage induced by SPF. Furthermore, the same dose of isopsoralen was found to cause more severe liver damage than psoralen. Altogether, psoralen and isopsoralen were identified as the major components responsible for PF-induced hepatotoxicity. According to recent studies, psoralen penetrates the phospholipid cellular membranes and is inserted between the pyrimidines of deoxyribonucleic acid (DNA). Psoralens are initially biologically inert and acquire photoreactivity upon exposure to certain classes of electromagnetic radiation, such as ultraviolet light. Once activated, psoralens form mono- and di-adducts with DNA, leading to marked cell apoptosis (Panagis et al., 2024). Psoralen- and isopsoralen-induced cytotoxic effects were associated with putative core targets (i.e., Fn1, Thbs1, and Tlr2) and multiple signaling pathways (e.g., PI3K-Akt, MAPK, and TNF pathways) (Chen et al., 2023).

5. Conclusion

In the present study, SULT1E1 overexpression was found to reverse liver damage in each treatment group. Moreover, the severity of liver damage was found to be significantly lower in the rAAV8-SULT1E1 groups than that in the rAAV8-empty groups. Liver damage due to isopsoralen was stronger than that caused by psoralen at the same dose. Thus, SULT1E1 is an important target gene for liver damage induced by SPF. Targeting the FXR-SULT1E1 pathway may represent a promising therapeutic strategy against SPF-induced cholestasis and hepatic damage. The results suggested that the estrogen levels of patients should be examined to individualize the use of SPF to avoid possible adverse effects. Overall, HNF4α may not be the upstream target of psoralen and isopsoralen that act on the FXR-SULT1E1 signaling pathway.

CRediT authorship contribution statement

Yu Wu: Conceptualization, Data curation, Project administration, Validation, Writing – original draft, Writing – review & editing. **Yan Xu:** Writing – review & editing. **Hao Cai:** Supervision, Writing – review & editing. **ZhengYing Hua:** Visualization, Writing – original draft. **Meimei Luo:** Data curation, Formal analysis. **Leitao Hu:** Data curation, Formal analysis. **Nong Zhou:** Supervision, Writing – review & editing. **Xinghong Wang:** Writing – review & editing. **Weidong Li:** Conceptualization, Data curation, Project administration, Validation, Writing – original draft, Writing – review & editing. In our earlier proofreading comments, we indicated to remove the redundant 'Declaration of competing interest' that appeared multiple times. This correction was not intended to eliminate all conflict of interest statements, only the duplicated ones.

Declaration of competing interest

The authors declare that they have no known competing finacial interests or personal relationships that could have appeared to influence the work reported in this paper.

Acknowledgments

This work was supported by the National Natural Science Foundation of China (81973484 and 82304736) and the 2022 Natural Science Foundation of Nanjing University of Chinese Medicine (XZR2021085).

References

Barbosa, A. C. S., Feng, Y., Yu, C., Huang, M., & Xie, W. (2019). Estrogen sulfotransferase in the metabolism of estrogenic drugs and in the pathogenesis of diseases. *Expert Opinion on Drug Metabolism & Toxicology, 15*(4), 329–339.

Bechmann, L. P., Kocabayoglu, P., Sowa, J. P., Sydor, S., Best, J., Schlattjan, M., ... Canbay, A. (2013). Free fatty acids repress small heterodimer partner (SHP) activation and adiponectin counteracts bile acid-induced liver injury in superobese patients with nonalcoholic steatohepatitis. *Hepatology, 57*(4), 1394–1406.

Bi, Y. N., Li, Z., Zhou, K., Zhao, X. Y., Shi, H., & Zheng, L. (2015). Influence of Bakuchiol on liver function and bile acid transporters BSEP and NTCP in mouse. *Journal of Tianjin University of Traditional Chinese Medicine, 34*(4), 222–225.

Chen, S., Guo, W., Liu, H., Zheng, J., Lu, D., Sun, J., ... Liu, T. (2023). Mechanistic study of cytochrome P450 enzyme-mediated cytotoxicity of psoralen and isopsoralen. *Food and Chemical Toxicology, 180*, 114011.

Chiang, J. Y. L. (2013). Bile acid metabolism and signaling. *Comprehensive Physiology, 3*(3), 1191–1212.

Choi, J. S., & Song, J. (2009). Effect of genistein on insulin resistance, renal lipid metabolism, and antioxidative activities in ovariectomized rats. *Nutrition, 25*(6), 676–685.

Costarelli, V., & Sanders, T. A. B. (2002). Plasma deoxycholic acid concentration is elevated in postmenopausal women with newly diagnosed breast cancer. *European Journal of Clinical Nutrition, 56*(9), 925–927.

Duan, J., Dong, W., Xie, L., Fan, S., Xu, Y., & Li, Y. (2020). Integrative proteomics-metabolomics strategy reveals the mechanism of hepatotoxicity induced by *Fructus Psoraleae*. *Journal of Proteomics, 221*, 103767.

Fashe, M., Hashiguchi, T., Yi, M., Moore, R., & Negishi, M. (2018). Phenobarbital-induced phosphorylation converts nuclear receptor RORα from a repressor to an activator of the estrogen sulfotransferase gene Sult1e1 in mouse livers. *FEBS Letters, 592*(16), 2760–2768.

Gao, C., Liu, C., Wei, Y., Wang, Q., Ni, X., Wu, S., ... Hao, Z. (2023). The acute oral toxicity test of ethanol extract of salt-processed *Psoraleae Fructus* and its acute hepatotoxicity and nephrotoxicity risk assessment. *Journal of Ethnopharmacology, 309*, 116334.

Gao, S., Duan, X., Wang, X., Dong, D., Liu, D., Li, X., ... Li, B. (2013). Curcumin attenuates arsenic-induced hepatic injuries and oxidative stress in experimental mice through activation of Nrf2 pathway, promotion of arsenic methylation and urinary excretion. *Food and Chemical Toxicology, 59*, 739–747.

Halilbasic, E., Claudel, T., & Trauner, M. (2013). Bile acid transporters and regulatory nuclear receptors in the liver and beyond. *Journal of Hepatology, 58*(1), 155–168.

Herraez, E., Gonzalez-Sanchez, E., Vaquero, J., Romero, M. R., Serrano, M. A., Marin, J. J. G., & Briz, O. (2012). Cisplatin-induced chemoresistance in colon cancer cells involves FXR-dependent and FXR-independent up-regulation of ABC proteins. *Molecular Pharmaceutics, 9*(9), 2565–2576.

Kasano-Camones, C. I., Takizawa, M., Ohshima, N., Saito, C., Iwasaki, W., Nakagawa, Y., ... Inoue, Y. (2023). PPARα activation partially drives NAFLD development in liver-specific *Hnf4a*-null mice. *The Journal of Biochemistry, 173*(5), 393–411.

Kleven, M. D., Gomes, M. M., Wortham, A. M., Enns, C. A., & Kahl, C. A. (2018). Ultrafiltered recombinant AAV8 vector can be safely administered *in vivo* and efficiently transduces liver. *PLoS One, 13*(4), e0194728.

Kodama, S., Hosseinpour, F., Goldstein, J. A., & Negishi, M. (2011). Liganded pregnane X receptor represses the human sulfotransferase SULT1E1 promoter through disrupting its chromatin structure. *Nucleic Acids Research, 39*(19), 8392–8403.

Liao, Y. N., Zhao, K. L., & Guo, H. W. (2024). Application and challenges of network pharmacology research in traditional Chinese medicine. *Chinese Traditional and Herb Drugs, 55*(12), 4204–4213.

Lim, S. H., Ha, T. Y., Ahn, J., & Kim, S. (2011). Estrogenic activities of *Psoralea* corylifolia L. seed extracts and main constituents. *Phytomedicine, 18*(5), 425–430.

Marrone, J., Soria, L. R., Danielli, M., Lehmann, G. L., Larocca, M. C., & Marinelli, R. A. (2016). Hepatic gene transfer of human aquaporin-1 improves bile salt secretory failure in rats with estrogen-induced cholestasis. *Hepatology, 64*(2), 535–548.

Meng, Q., Chen, X., Wang, C., Liu, Q., Sun, H., Sun, P., ... Liu, K. (2015). Protective effects of alisol B_{23}-acetate *via* farnesoid X receptor-mediated regulation of transporters and enzymes in estrogen-induced cholestatic liver injury in mice. *Pharmaceutical Research, 32*(11), 3688–3698.

Mulorz, J., Spin, J. M., Beck, H. C., Tha Thi, M. L., Wagenhäuser, M. U., Rasmussen, L. M., ... Steffensen, L. B. (2020). Hyperlipidemia does not affect development of elastase-induced abdominal aortic aneurysm in mice. *Atherosclerosis, 311*, 73–83.

Okada, K., Warabi, E., Sugimoto, H., Horie, M., Gotoh, N., Tokushige, K., ... Shoda, J. (2013). Deletion of Nrf2 leads to rapid progression of steatohepatitis in mice fed atherogenic plus high-fat diet. *Journal of Gastroenterology, 48*(5), 620–632.

Shi, Z., Gao, J., Pan, J., Zhang, Z., Zhang, G., Wang, Y., & Gao, Y. (2022). A systematic review on the safety of *Psoraleae Fructus*: Potential risks, toxic characteristics, underlying mechanisms and detoxification methods. *Chinese Journal of Natural Medicines, 20*(11), 805–813.

Soliman, A. M., Karam, H. M., Mekkawy, M. H., & Ghorab, M. M. (2020). Antioxidant activity of novel quinazolinones bearing sulfonamide: Potential radiomodulatory effects on liver tissues *via* NF-κB/PON1 pathway. *European Journal of Medicinal Chemistry, 197*, 112333.

Wang, S., Yuan, X., Lu, D., Guo, L., & Wu, B. (2017). Farnesoid X receptor regulates SULT1E1 expression through inhibition of PGC1α binding to HNF4α. *Biochemical Pharmacology, 145*, 202–209.

Wang, Y., Zhang, H., Jiang, J. M., Zheng, D., Chen, Y. Y., Wan, S. J., ... Xu, H. X. (2019). Hepatotoxicity induced by psoralen and isopsoralen from *Fructus Psoraleae*: Wistar rats are more vulnerable than ICR mice. *Food and Chemical Toxicology, 125*, 133–140.

Wu, Y., Min, L., Xu, Y., Liu, H., Zhou, N., Hua, Z., ... Li, W. (2022). Combination of molecular docking and liver transcription sequencing analysis for the evaluation of salt-processed *Psoraleae Fructus*-induced hepatotoxicity in ovariectomized mice. *Journal of Ethnopharmacology, 288*, 114955.

Xin, D., Wang, H., Yang, J., Su, Y. F., Fan, G. W., Wang, Y. F., ... Gao, X. M. (2010). Phytoestrogens from *Psoralea* corylifolia reveal estrogen receptor-subtype selectivity. *Phytomedicine, 17*(2), 126–131.

Xu, K., Sha, Y., Wang, S., Chi, Q., Liu, Y., Wang, C., & Yang, L. (2019). Effects of Bakuchiol on chondrocyte proliferation *via* the PI3K-Akt and ERK1/2 pathways mediated by the estrogen receptor for promotion of the regeneration of knee articular cartilage defects. *Cell Proliferation, 52*(5) e12666.

Zhang, X. Y., Wang, D. N., Chai, X., Yu, H. J., Cui, Y., & Wang, Y. F. (2024). Illumination on quality features of *Psoraleae Fructus* and its application in detoxification process. *Chinese Traditional and Herb Drugs, 55*(8), 2784–2791.

Zhao, X., Fu, J., Xu, A., Yu, L., Zhu, J., Dai, R., ... Wang, H. (2015). Gankyrin drives malignant transformation of chronic liver damage-mediated fibrosis *via* the Rac1/JNK pathway. *Cell Death & Disease, 6*(5), e1751.

Zincarelli, C., Soltys, S., Rengo, G., & Rabinowitz, J. E. (2008). Analysis of AAV serotypes 1–9 mediated gene expression and tropism in mice after systemic injection. *Molecular Therapy, 16*(6), 1073–1080.